

Electronic excitation transfer in Lennard-Jones fluid: Comparison between approaches based on molecular dynamics simulation and the many-body Smoluchowski equation

T. Bandyopadhyay

Citation: *The Journal of Chemical Physics* **106**, 8355 (1997); doi: 10.1063/1.473897

View online: <http://dx.doi.org/10.1063/1.473897>

View Table of Contents: <http://scitation.aip.org/content/aip/journal/jcp/106/20?ver=pdfcov>

Published by the [AIP Publishing](#)

Articles you may be interested in

[Self-diffusion coefficient of two-center Lennard-Jones fluids: Molecular simulations and free volume theory](#)
J. Chem. Phys. **130**, 024503 (2009); 10.1063/1.3054139

[NMR relaxation parameters of a Lennard-Jones fluid from molecular-dynamics simulations](#)
J. Chem. Phys. **123**, 034503 (2005); 10.1063/1.1955447

[Simulation of environmental effects on coherent quantum dynamics in many-body systems](#)
J. Chem. Phys. **120**, 6863 (2004); 10.1063/1.1651472

[Corresponding states law and molecular dynamics simulations of the Lennard-Jones fluid](#)
J. Chem. Phys. **115**, 6623 (2001); 10.1063/1.1396674

[Interfacial tension behavior of binary and ternary mixtures of partially miscible Lennard-Jones fluids: A molecular dynamics simulation](#)
J. Chem. Phys. **110**, 8084 (1999); 10.1063/1.478710



Electronic excitation transfer in Lennard-Jones fluid: Comparison between approaches based on molecular dynamics simulation and the many-body Smoluchowski equation

T. Bandyopadhyay

Chemistry Division, Bhabha Atomic Research Centre, Trombay, Mumbai 400 085, India

(Received 28 October 1996; accepted 19 February 1997)

Molecular dynamics simulations were performed to study the kinetics of long-range irreversible/reversible electronic excitation transfer in a Lennard-Jones fluid where the translationally mobile chromophores are thought to be embedded. The simulations are based on the Förster master rate equation approach which can be rederived from a stochastic Liouville formalism for excitation transfer between two identical chromophores in the weak dipole–dipole coupling regime. For energy transfer between two dissimilar partners, rate equations utilized are obtained from the first principle. The simulated kinetic results in this regime are then compared with the reaction-diffusion theoretical framework for excitation transfer. The theory is based on a many-body Smoluchowski equation for the reactant molecule reduced distribution function and makes use of a superposition approximation to truncate the hierarchy of equations. The comparison of the results show the scope and utility of the theoretical approach in the high friction limit when it is solved for the absorbing boundary condition at contact. In the low friction limit, like collisional quenching, the present reaction-diffusion formalism is found to perform poorly. When the stochastic Liouville equation in the strong dipolar coupling regime is solved combined with the molecular dynamics trajectories, the time dependent reaction probability of the donor shows oscillatory behavior and the diffusion coefficient of the medium has been found to have but little effect on this. © 1997 American Institute of Physics. [S0021-9606(97)50320-5]

I. INTRODUCTION

Since the early work of Förster¹ and Dexter² there have been many developments in the theory of electronic excitation energy transfer between the donor–acceptor pair. The transfer mechanisms are incorporated through different forms of donor–acceptor distance-dependent transfer rates. The one that is of our consideration here is the long-range dipolar interaction mediated transfer. It is generally argued that the diffusion can affect the rates of fast reaction such as electronic energy transfer. Rice³ has recently reviewed diffusion-controlled energy transfer reactions. The necessary condition for energy to be transferred from a donor to an acceptor is that there should be an overlap of donor emission spectrum and acceptor absorption spectrum. On the other hand, one naively expects that in systems where the ¹S levels of the donor and the acceptor molecule are closely located and there is a overlap between the acceptor fluorescence and the donor absorption spectra, the reverse transfer process gains its importance. This is more so in the case of donor–donor energy transfer. However, despite the ubiquity and importance of reversibility in diffusion-influenced reactions such processes have only recently attracted much work.

Several authors^{4–7} have recently addressed the problem of reversible energy transfer. In Ref. 5 Burshtein and Lukzen have solved both the integral and differential variant of the encounter theory to find the kinetics of reversible energy transfer. The crucial point that has been addressed by these authors is the correlation between lifetime of the donor–acceptor partners with the duration of encounter between them. It has been shown in Ref. 5, that the effective rate

constant becomes negative at a long time reflecting the reverse transfer of energy conserved at a long-living acceptor to the short-lived partner that produces delayed luminescence. Such phenomena occurs from several recontacts between partners during encounter. It has also been shown in Refs. 4 and 5 that only the memory function formalism like integral encounter theory is capable to deal with delayed luminescence events. Sienicki and Mattice⁶ used a model based on Markovian and non-Markovian theory of energy transfer to account for the forward and reverse energy transfer in the presence of energy migration and correlation in rigid solution.

In Ref. 7, following Lee and Karplus,⁸ we have obtained a set of coupled dynamic equations for the reduced distribution functions of the reactant molecules (modulated by diffusion) between the forward and the reverse steps. This theory is based on an infinite hierarchy of the many-body Smoluchowski equation which is truncated at the pair distribution level using a superposition approximation. Szabo⁹ has shown the relationship between Lee and Karplus theory and the Smoluchowski-type approach as generalized to include the back reaction. With a view towards treating long-range interaction mediated energy transfer kinetics, this formalism was used to include the unimolecular decay pathways of the reactants.⁷ Physical features for the competition of relative motion and reaction in excitation transfer are established in Ref. 7. We have shown therein that the reversibility has the effect of making donor decay kinetics different from the irreversible forward transfer kinetics. The theory that had been developed in Ref. 7 was not aimed at describing the delayed

luminescence or trapping related energy conservation phenomena.^{4,5} Rather the theoretical model in Ref. 7 essentially describes a transient fluorescence quenching kinetics duo to long-range excitation energy transfer in the presence of reverse transfer that becomes indispensable for the situation such that the acceptor fluorescence overlaps with the donor absorption spectra. The distance dependent transfer rates (see below) is continuous (i.e., nonzero) in space rendering the bidirectional transfer process continuous in space and time. This is in sharp contrast to the encounter theory^{4,5} where the distance dependent transfer rates differ from zero only within a certain intermolecular diameter.

Recently Westlund and Wennerström¹⁰ have developed a stochastic Liouville formalism that treats the energy transfer process on an equal footing as other relaxation processes. The stochastic Liouville equation (SLE) developed by these authors includes the effects due to molecular dynamic events e.g., rotation. Subsequently, an algorithm is developed by Fedchenia and Westlund¹¹ to solve the SLE for energy transfer between identical luminescent pair of molecules in the presence of rotational dynamics. The fluctuating part of the SLE were obtained from Brownian dynamics simulation.¹¹ Results were obtained for both weak and strong coupling regime in the absence of solvent relaxation effects as well as in the absence of vibrational coupling amongst the fluorophores. The general formalism adopted by these authors^{10,11} essentially advocates reversible transfer of excitation energy between a donor–donor pair influenced by diffusion. This is clearly manifested by the oscillatory behavior of the fluorophore survival probability in the strong coupling regime. An alternative to this rotational dynamics approach is the Monte Carlo simulation of donor–donor excitation jump¹² under the influence of dipolar coupling or else solving the kinetic master equation after the rotational trajectories are being obtained from Brownian dynamics simulation.¹³

However, our intention in this work is the influence of translational dynamics on the energy transfer kinetics.

Dong, Baros, and Andre¹⁴ have recently elaborated on a molecular dynamics simulation method based on the first principle for a model fluorescence quenching kinetics in a hard sphere liquid. While comparing the simulation data with the simplest version of the Smoluchowski theory using an absorbing boundary condition (BC) and ignoring the solvent influence on the potential of mean force, large discrepancy at short times has been found, that has been attributed to the memory effects. Subsequently, Zhou and Szabo¹⁵ have compared the simulation data using a refined version of the Smoluchowski theory incorporating the potential of mean force. The resulting equation was solved by radiative BC. Excellent agreement between theory and simulation was obtained for a wide range of quencher concentration suggesting that memory effects are unimportant.¹⁵

In a more recent work¹⁶ we have verified the refined version of the Smoluchowski theory when comparing with the simulated results of complicated light intensity effects on diffusion-influenced fluorescence quenching kinetics in a hard sphere liquid. Again memory effects are found to be unimportant. In Ref. 16 as well as in this work the theory is

based on a hierarchical system of the many-body Smoluchowski equation for the reactant molecule distribution function.⁸ The success of the refined version of theory over its primitive counterpart can be justified by the fact that Langevin dynamics with an absorbing BC in the high friction limit (in dense liquid) reduces to the Smoluchowski equation with the radiative BC.¹⁵ In these studies^{14–16} the coupling of translational and reactive dynamics were investigated where the reaction was thought to be caused by the collisions between the reactants.

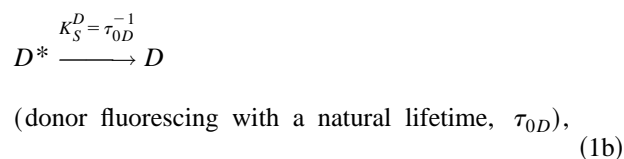
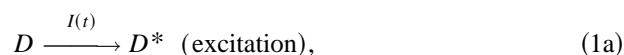
It is the purpose of the present work to verify the reaction-diffusion formalism⁷ in the situation where the quenching process is not merely collisional, but due to long-range energy transfer interaction and the transfer process is either unidirectional (irreversible) or bidirectional (reversible) between a donor–acceptor pair in a Lennard-Jones fluid. To achieve this we have utilized the SLE scheme^{10,11} in the weak dipole–dipole coupling limit (see below) for the donor–donor case of reversible energy transfer and have incorporated the translational mobility of the fluorophores into the scheme. For the donor–acceptor case of irreversible/reversible energy transfer we have utilized the rate equations⁴ obtained from the first principle. The translational trajectories of the reactants are simulated by molecular dynamics (MD) simulation. The results are then compared in the weak Förster regime with those obtained from irreversible and reversible energy transfer kinetics based on the many-body Smoluchowski equation approach. The unified derivation of the generalized Brownian motion theory¹⁷ illustrates that the Liouville equation ultimately reduces to transport equations. That is, the associated equation of motion, for the configurational distribution function with the “position Langevin equation” is the well known Smoluchowski equation. This increases our confidence in undertaking this work.

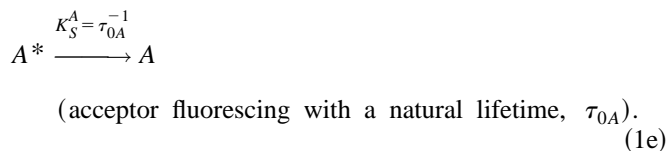
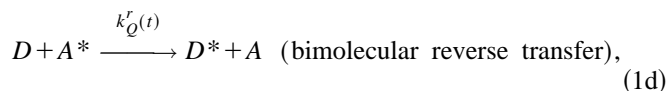
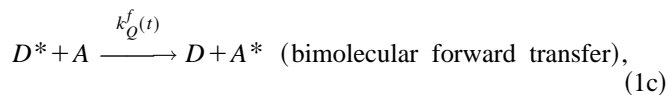
In Sec. II we will present the theoretical treatment for a model reversible energy transfer kinetics. There we will briefly outline the main theoretical equations of diffusion-influenced reversible reaction.⁷ The SLE approach of excitation transfer and its reduction to the Förster master rate equation¹⁰ will also be outlined in this section. In Sec. III we will discuss the methods of computation. The results will be compared and discussed in Sec. IV and finally in Sec. V we will present the main conclusions of this work.

II. THEORETICAL TREATMENT

A. The reaction-diffusion equation

Donor–acceptor bidirectional energy transfer kinetics can be described by the following general reaction scheme:





We also consider an isothermal homogenous liquid solution where the reactants are embedded and the solvent is supposed to be chemically inert. The reaction vessel is large enough to avoid any surface effects.

Following Lee and Karplus,⁸ in Ref. 7 we have obtained an infinite hierarchy of equations for the reactive reduced distribution functions in the many-body Smoluchowski equation framework and truncated this hierarchy at the pair distribution level using the superposition approximation. Following this the rate law for reaction schemes (1a)–(1e) reads

$$\frac{d}{dt} [D^*] = -K_S^D [D^*] - k_Q^f(t) [D^*] [A] + k_Q^r(t) [D] [A^*] \quad (2)$$

and

$$\frac{d}{dt} [A^*] = -K_S^A [A^*] - k_Q^r(t) [D] [A^*] + k_Q^f(t) [D^*] [A]. \quad (3)$$

The first terms on the right-hand side of Eqs. (2) and (3) correspond to the emission from the excited donor and the excited acceptor (with a rate, K_S^j , $j = D$ or A), respectively, in the absence of energy transfer events. The second terms represent radiationless energy transfer, from the donor to the acceptor with a rate $k_Q^f(t)$ in Eq. (2), and from the acceptor to the donor with a rate $k_Q^r(t)$ in Eq. (3). The third terms in these equations are for the increase in concentration of the excited fluorophores for the opposite reverse process. The time-dependent quenching rate constants depend on the details of the time evolution of distribution functions of the reactant molecules and obtained as such from this hierarchical approach. They are given by

$$k_Q^f(t) = \int dr 4\pi r^2 S_{DA}(r) \rho_{D^*A}(r, t) \quad (4)$$

and

$$k_Q^r(t) = \int dr 4\pi r^2 S_{AD}(r) \rho_{A^*D}(r, t). \quad (5)$$

$S_{DA}(r)$ and $S_{AD}(r)$ are the distance dependent transfer rate between the donor and the acceptor, which according to Förster isotropic dipolar interaction mechanism is given by

$$S_{DA} = \tau_{0D}^{-1} \left(\frac{R_{0f}}{r_{DA}} \right)^6, \quad (6)$$

$$S_{AD} = \tau_{0A}^{-1} \left(\frac{R_{0r}}{r_{AD}} \right)^6. \quad (7)$$

R_{0f} is the Förster radius for the forward transfer from the donor to the acceptor and R_{0r} is the same for the reverse transfer from the acceptor to the donor. $\rho_{\alpha\beta}(r, t)$ that appears in Eqs. (4) and (5) is the nonequilibrium pair distribution function between α and β molecules. The procedure developed in Ref. 7 leads to the following equations for the time evolution of $\rho_{\alpha\beta}(r, t)$:

$$\begin{aligned} \frac{\partial}{\partial t} \rho_{D^*A}(r, t) &= L_{D^*A} \rho_{D^*A}(r, t) - S_{DA}(r) \rho_{D^*A}(r, t) + S_{AD}(r) \frac{g(r)}{[D^*]} \\ &\times \left\{ \frac{[D]}{[A]} C_A^0 - C_D^0 \right\} + S_{AD}(r) \rho_{D^*A}(r, t) + \frac{[A^*]}{[D^*]} k_Q^r(t) \\ &\times C_D^0 [g(r) - \rho_{D^*A}(r, t)] + K_S^A \left\{ \frac{C_A^0}{[A]} g(r) - \rho_{D^*A}(r, t) \right\} \\ &- \left\{ K_S^A \frac{[A^*]}{[A]} + K_Q^r(t) \frac{[D][A^*]}{[A]} - k_Q^f(t) [D^*] \right\} \rho_{D^*A}(r, t), \end{aligned} \quad (8)$$

and

$$\begin{aligned} \frac{\partial}{\partial t} \rho_{A^*D}(r, t) &= L_{A^*D} \rho_{A^*D}(r, t) - S_{AD}(r) \rho_{A^*D}(r, t) + S_{DA}(r) \frac{g(r)}{[A^*]} \\ &\times \left\{ \frac{[A]}{[D]} C_D^0 - C_A^0 \right\} + S_{DA}(r) \rho_{A^*D}(r, t) + \frac{[D^*]}{[A^*]} k_Q^f(t) \\ &\times C_A^0 [g(r) - \rho_{A^*D}(r, t)] + K_S^D \left\{ \frac{C_D^0}{[D]} g(r) - \rho_{A^*D}(r, t) \right\} \\ &- \left\{ K_S^D \frac{[D^*]}{[D]} + k_Q^f(t) \frac{[A][D^*]}{[D]} - k_Q^r(t) [A^*] \right\} \rho_{A^*D}(r, t). \end{aligned} \quad (9)$$

The Smoluchowski operator that appears in Eqs. (8) and (9) is given by

$$L_{\alpha\beta} = \left(\frac{\partial}{\partial r} + \frac{2}{r} \right) D_{\alpha\beta}(r) \left[\frac{\partial}{\partial r} + \frac{1}{k_B T} \frac{\partial}{\partial r} U_{\alpha\beta}(r) \right]. \quad (10)$$

$D_{\alpha\beta}(r)$ is the r -space dependent relative diffusion coefficient between α and β molecules. We assume that hydrodynamic interactions are absent and the relative diffusion coefficient is equal to twice the self-diffusion constant. The solvent influences on the potential of the mean force, $U(r)$, is related to the radial distribution function $g(r)$ through $\exp[-U(r)/k_B T] = g(r)$, where k_B is the Boltzmann constant and T is the absolute temperature. C_A^0 and C_D^0 that appear in Eqs. (8) and (9) are the total number density of the fluorophore molecules in the ground and the excited states.

In a general way, we are interested in the time scale longer than the momentum relaxation time scale and we use a superposition of diffusion and reaction, the latter being introduced through a space-dependent chemical rate constant, $k(r)$. This consideration leads for a simple reaction such as $\alpha + \beta \rightarrow \gamma$, to

$$\frac{\partial \rho_{\alpha\beta}}{\partial t} = L_{\alpha\beta} \rho_{\alpha\beta} - k(r) \rho_{\alpha\beta}.$$

This basic reaction-diffusion equation is the key to study the coupling between translational and reactive dynamics for a Smoluchowski model. Thus Eqs. (8) and (9) are the reaction-diffusion equations. The complexity of these equations is a natural consequence of the many-body Smoluchowski approach and arises due to the fact that the survival probability is obtained directly as absolute number density of the reactant concerned.

Equations (2) and (3) along with Eqs. (8) and (9) form a coupled set of dynamic equations between the forward and the reverse processes that is to be solved given the forward and reverse quenching rate coefficients [cf. Eqs. (4) and (5), respectively]. The solution gives kinetic information on the instantaneous value of the number density of $[D^*]$ and $[A^*]$.

For energy transfer between identical fluorophores i.e. donor-donor case we have $K_S^D = K_S^A$, $R_{0f} = R_{0r}$, and $g_{D^*A}(r) = g_{A^*D}(r) = g(r)$. The situation replicates a typical fluorescence lifetime measurement experiment of a fluorophore. A certain number of donor molecules are excited by a very short (δ like) light flash of low intensity. The remaining second group of donor molecules that remains in the ground state acts as acceptor. The total excitation that remains in either group of donors will decay exponentially with a rate constant K_S^D . This can be verified⁷ by adding Eq. (2) with Eq. (3) and taking $K_S^D = K_S^A$.

Up to now we were considering the kinetic equations governing the time evolution of the donor excitation. We now turn to discuss the Förster master rate equations that we will utilize in the MD simulations.

B. The Förster master rate equations

In the Liouville formalism of excitation transfer¹⁰ one donor and one acceptor is thought to be embedded in a solution and each of the chromophores is assumed to have only one excited state, $|1\rangle$ and a ground state, $|0\rangle$. The time evolution of the combined state of the system is governed by the Liouville equation of motion,¹⁰

$$\frac{\partial}{\partial t} P_A \otimes P_D = -i\{\mathcal{L}_A + \mathcal{L}_D + \mathcal{L}_{AD}\} P_A \otimes P_D. \quad (11)$$

$P_A \otimes P_D$ is the direct product of the two electron density operators;¹⁸ P_A and P_D designates the combined state of the system. It is to be mentioned that by the suffix A and D we designate acceptor and donor, respectively, that can either be in the ground or in the excited state determined by the matrix elements of P_A and P_D (see below). The Liouville operators \mathcal{L}_A and \mathcal{L}_D are the superoperators for the individual

chromophores. The coupling \mathcal{L}_{AD} between A and D is obtained from time-dependent dipole-dipole interaction Hamiltonian $H^{DD}(t)$ as a derivation superoperator.¹⁸ $H^{DD}(t)$ is given by

$$H^{DD}(t) = \frac{\mu_A \mu_D}{4\pi\epsilon_0 r_{AD}^3(t)}, \quad (12)$$

where μ_A and μ_D are the transition dipole operators, ϵ_0 is vacuum permittivity. The stochastic fluctuating part in the expression for $H^{DD}(t)$ is arising out of the translational diffusion between the two chromophores embedded in the fluid solution and enters into the formalism through a time-dependent inter chromophore distance $r_{AD}(t)$. In the Liouville operator formalism, the eigenvalues are energy difference or the transition frequencies between the state levels.

The eigenoperators of the Liouville $i\mathcal{L}_j$ ($j=A$ or D) have four matrix elements, they are

$$P_1^j = |0\rangle\langle 0|, P_2^j = |1\rangle\langle 1|, P_3^j = |0\rangle\langle 1|, P_4^j = |1\rangle\langle 0|. \quad (13)$$

The corresponding eigenvalues (in frequency units) for them are

$$\lambda_1 = 0, \lambda_2 = \tau_{0j}^{-1}, \lambda_3 = -i\omega_j - \frac{1}{T_{2j}}, \lambda_4 = i\omega_j - \frac{1}{T_{2j}}. \quad (14)$$

τ_{0j} is the natural lifetime of the fluorophore j in the absence of the quencher, ω_j is the ΔE energy gap between the ground and the excited state of the fluorophore j , and $1/T_{2j}$ is the width of the Lorentzian absorption peak at ω_j .^{18(a)} These eigenvalues are obtained assuming that the vibrational coupling in between the fluorophores and the fluorophores with the medium are absent. ω_j, T_2 are intimately related with the Förster radius R_0 .

By Eqs. (11)–(13) we arrived at a 16-dimensional system because of the 16 possible combinations of the P_i^j ($j=A$ or D , $i=1, \dots, 4$) that generates the combined state of the system.¹⁰ This is certainly a much complicated situation. However, we are primarily interested in the time evolution of the excited state of the donor and the ground state of the acceptor, $P_1^A P_2^D(t)$ given that at $t=0$, $P_1^A P_2^D(0) = 1$. Keeping this in mind the 16-dimensional system can be reduced to a much simpler 4×4 form by the assumption¹⁰ that the dipolar coupling pertaining to \mathcal{L}_{AD} is weak relative to the excitation energy. In such a situation the states of the combined systems are

$$\chi_1 \equiv P_1^A P_2^D, \chi_2 \equiv P_2^A P_1^D, \chi_3 \equiv P_3^A P_4^D, \chi_4 \equiv P_4^A P_3^D, \quad (15)$$

and the equation of motion reads as

$$\frac{d}{dt} \chi(t) = -i\mathcal{L} \chi(t), \quad (16)$$

where χ is the vector of the four elements given in Eq. (15) and $\mathcal{L} = \mathcal{L}_A + \mathcal{L}_D + \mathcal{L}_{AD}$. In the language of SLE, χ is a function of the time variable, t and the multidimensional coordinate summarizing all the positions and momenta of a point

particle system. In that context Eq. (16) is the SLE that we intend to solve with the Liouville matrix \mathcal{L} , given by¹⁰

$$\mathcal{L} = \begin{bmatrix} -1/\tau_{0A} & 0 & i/\sqrt{2}H & -i/\sqrt{2}H \\ 0 & -1/\tau_{0D} & -i/\sqrt{2} & i/\sqrt{2}H \\ i/\sqrt{2}H & -i/\sqrt{2}H & iC & 0 \\ -i/\sqrt{2}H & i/\sqrt{2}H & 0 & -iC^* \end{bmatrix},$$

where $C = -(1/T_2) - i\delta$; $(1/T_2) = (1/T_{2A}) - (1/T_{2D})$; $\delta = \omega_D - \omega_A$; and the off-diagonal term H is as given by Eq. (12). The stochastic time dependence is due to random donor–acceptor distance $r_{DA}(t)$ that appears in Eq. (12). The above equations are quite general and the acceptor can either be the same species as the donor, which is called the donor–donor energy transfer, or else it can also be different species; the donor–acceptor case. Obviously for the donor–donor case $\tau_{0A} = \tau_{0D}$ and $\delta = 0$. In what immediately follows we will first consider the donor–donor case.

To make the computational algorithm simpler this matrix can be further decomposed into a diagonal (\mathcal{L}_0) and an off-diagonal (\mathcal{L}_1) part¹¹

$$\frac{d}{dt} \chi(t) = -[\mathcal{L}_0 + iH^{DD}(t)\mathcal{L}_1]\chi(t). \quad (17)$$

The formal solution of the matrix Eq. (17) is

$$\chi(t_{i+1}) = e^{[\mathcal{L}_0 + iH^{DD}(t_i)\mathcal{L}_1]\Delta t} \chi(t_i), \quad (18)$$

where $\Delta t = (t_{i+1} - t_i)$, is the temporal step size that one uses for calculating the time dependent dipolar coupling term $H^{DD}(t)$, $\chi(t_{i+1})$ is the column vector containing elements of Eq. (15) at time t_{i+1} . Equation (18) can be further simplified by noting that¹¹

$$e^{[\mathcal{L}_0 + iH^{DD}(t_i)\mathcal{L}_1]\Delta t} = e^{\mathcal{L}_0 \Delta t/2} e^{iH^{DD}(t_i)\mathcal{L}_1 \Delta t} e^{\mathcal{L}_0 \Delta t/2} + O(\Delta t^3). \quad (19)$$

Equation (19) is basically a finite difference scheme provided and all matrix exponentials those appeared in Eq. (19) are given in Ref. 11. It can be readily seen from Eq. (19) that in the absence of energy transfer i.e., when the dipole–dipole interaction Hamiltonian is zero, the solution of this equation gives the natural lifetime of the fluorophore concerned. Put in other words, when $H^{DD}(t)$ is nonzero the density vector of the four elements, presented in Eq. (15) will couple with each other and in such situation the temporal evolution of $\chi_1(t)$ will represent the energy flow from the donor to acceptor along with its natural fluorescence decay.

Equation (18) is the working expression. Starting with $\chi_1 = 1$ and $\chi_{2,3,4} = 0$, i.e., the donor is initially in the excited state and the acceptor is in the ground state, the values of the χ matrix elements are obtained at time t_{i+1} using Eq. (18) knowing the values of these along with the value of the dipolar coupling term at the previous step. Where the time dependent dipolar coupling elements are to be obtained from the MD simulations. It is to be noted that these equations are developed for the donor–donor energy transfer kinetics. We are interested in the temporal profile of the donor excited state that appears as a time-correlation function, $\langle \chi_1(t) | \chi_1(t_0) \rangle$ in the formalism and designates an ensemble

averaged survival probability of the donor. The other correlation function, $\langle \chi_2(t) | \chi_1(t_0) \rangle$ represents the temporal evolution of the second group of the donor that receives excitation energy from the first group of donor (and not from the external illumination). It is to be noted that for a donor–donor case, experimentally observable quantity is the sum of these two correlation functions which represents natural decay of the donor.⁷ As can be seen from Eq. (18) that in this way of solving the SLE equation of energy transfer, one is actually mixing the four density vectors of Eq. (15) from one time step to the other. That is, if we assume that the contributions of the density vectors, χ_3 and χ_4 is only negligible, then the population density of the states χ_1 and χ_2 couples with each other at each time step. It is in this sense, the *reversible* dynamics of energy transfer process is implicit in this formalism. This can be further verified by the fact that in the absence of natural decay, the sum of the two correlation functions, $\langle \chi_1(t) | \chi_1(t_0) \rangle$ and $\langle \chi_2(t) | \chi_1(t_0) \rangle$ will equate to 1, since in that case excitation energy has to be in one of the two chromophores.

The main purpose and the scope of the present work is to compare the MD simulation based results with those obtained from the coupled set of reaction-diffusion equations that has been described earlier. However, the SLE approach (that is to be combined with the MD simulation techniques) we have been considering until now, cannot be as such used for this comparison because of the following reasons.

First, the input parameters to the above SLE formalism are the natural lifetime of the donor; the resonance frequency and the assumed Lorentzian line width at the resonance frequency; and the time-invariant part of the dipole–dipole interaction Hamiltonian, $\mu_A \mu_D / 4\pi\epsilon_0$. The Förster rate of energy transfer, $S(r)$ that we use in the reaction-diffusion equation includes the factor R_0 which is intimately related to the input parameters essential for the SLE formalism. For example, for a pair of identical fluorophores,

$$R_0^6 = \frac{3}{4} \left(\frac{ch}{\omega} \right)^6 \frac{T_2}{\tau_{cl}} f_b,$$

where c is the velocity of light, h is the Planck constant, τ_{cl} is the decay time of classical electronic oscillator, and f_b is oscillator strength of transition between the ground and the excited levels. A lack of knowledge of the precise wave functions of these two levels will prohibit the determination of the dipole matrix elements and therefore the oscillator strengths and eventually the R_0 factor cannot be directly determined from the input parameters of the SLE method. The situation is similar for the donor–acceptor case of energy transfer.

Secondly, the two mixed state of the density vector elements, namely χ_3 and χ_4 of Eq. (15) will carry a non-negligible amount of population density from the state χ_1 and χ_2 . On the other hand, in the reaction-diffusion formalism we have assumed that only the ground and excited state of the donor and the acceptor are relevant without any mixing between them that can lead to the states like χ_3 and χ_4 . Therefore, a direct comparison between the methods will be inadequate. Thirdly, one may leave the R_0 factor as a free

parameter to be adjusted by fitting with the SLE results. But for a complex reaction-diffusion coupled problem, like the one we are considering, this is certainly unwise.

The above algorithm of solving the SLE is adequate both in the “weak” and “strong” dipolar coupling regime. Also this algorithm is developed for the donor–donor case of reversible energy transfer. In the strong coupling regime, $(\langle [H^{DD}]^2 \rangle / 6D)^{1/2} \gg 1$, and the Förster rate approach is not valid.^{10,11} By weak coupling one means that in this regime ordinary time-dependent perturbation theory can be applied. As shown below the Förster master rate equation involving $S_{DA}(r)$ and $S_{AD}(r)$ is in principle valid in the weak coupling regime.¹⁰

In the weak coupling regime, $(1/\tau_{0j}) - C$ is much larger than $(i/\sqrt{2})H^{DD}$. In such a situation one can get the eigenvectors and eigenvalues from the perturbation theory. The perturbation analysis leads to the transformation of the Liouville matrix \mathcal{L} into two uncoupled submatrices. The basis vectors χ_1 and χ_2 are transformed into

$$\chi'_1 = \chi_1 + \kappa_1 \chi_3 + \kappa_1^* \chi_4$$

and

$$\chi'_2 = \chi_2 + \kappa_2 \chi_3 + \kappa_2^* \chi_4,$$

where κ is of the order of $|H/C| \ll 1$. The 4×4 matrix Eq. (16) now reduces¹⁰ into the 2×2 form given as

$$\frac{d}{dt} \begin{bmatrix} \chi'_1 \\ \chi'_2 \end{bmatrix} = \begin{bmatrix} -1/\tau_{0D} - W & W \\ W & -1/\tau_{0A} - W \end{bmatrix} \begin{bmatrix} \chi'_1 \\ \chi'_2 \end{bmatrix}, \quad (20)$$

where W is given by

$$W(r, t) = \frac{(|\mu_A||\mu_D|)^2}{[r(t)]^6} \left(\frac{T_2}{\delta^2 T_2^2 + 1} \right) \equiv \frac{1}{\tau_{0j}} \left(\frac{R_0}{r(t)} \right)^6.$$

Equation (20) along with the associated expressions for the rate W , at a given instant of time, is precisely the conventional Förster master rate theory. The time-dependence in the expression for Förster rate, W arises because the donor–acceptor distance is a random function of time. The probability that the donor is still excited at time t can be directly obtained from χ_1 after some ensemble averaging.

The forward and reverse transfer rates, W are equal in Eq. (20) that was obtained from Eq. (16). That is Eq. (20) describes the donor–donor case of reversible energy transfer and this is based on the SLE formalism. However, similar such expression for the process of energy redistribution and natural decay of a donor–acceptor pair can be written following the first principle.⁴ These rate equations are given by

$$\begin{aligned} \frac{d}{dt} N_{D^*} &= -\frac{1}{\tau_{0D}} N_{D^*} - W_f(r, t) N_{D^*} N_A \\ &\quad + W_r(r, t) N_{A^*} N_D, \\ \frac{d}{dt} N_{A^*} &= -\frac{1}{\tau_{0A}} N_{A^*} - W_r(r, t) N_{A^*} N_D \\ &\quad + W_f(r, t) N_{D^*} N_A. \end{aligned} \quad (21)$$

Here N_{D^*} and N_{A^*} , are the number of excited donor and acceptor molecules, respectively while N_D and N_A are their ground state population and $W_\alpha(r, t)$ ($\alpha = f, r$; that stands for the forward and reverse processes, respectively) is the Förster rate which is a random function of time $\{W_\alpha = (1/\tau_{0j}) \times [R_{0\alpha}/r(t)]^6\}$. It is to be noted that $(N_{D^*} + N_D)$ and $(N_{A^*} + N_A)$ are the total number of excited and ground state molecules of donor and acceptor, respectively. In the limit that κ is zero so that χ_3 and χ_4 do not couple to χ_1 and χ_2 , the information obtained from ensemble averaged and normalized N_{D^*} (or N_{A^*}) for $W_f = W_r$ is identical with χ_1 (or χ_2) [obtained from Eq. (20)] and they represent donor survival probability (or acceptor excitation probability). In other words Eq. (21) is quite general and can be readily reduced to similar form as Eq. (20) that has been rederived from a SLE formalism.¹⁰ When W is zero, once again Eqs. (20) and (21) give the natural lifetime of the donor as it should be.

In the next section for weak coupled limit ($\kappa = 0$) we will use Eq. (20) for the donor–donor case and Eq. (21) when the donor and acceptor molecules are dissimilar. In the strong coupled limit (κ is large) since the Förster rate is not valid, we use Eq. (18) developed for the donor–donor case.

III. METHODS OF COMPUTATION

A. Numerical solution of the reaction-diffusion equation

We need to solve the coupled sets of dynamic Eqs. (2) and (8) along with Eqs. (3) and (9), Eqs. (4) and (5) being common to them, to compare the results with those obtained from the Liouville formalism [cf. Eq. (20)] and from the first principle [cf. Eq. (21)] in which the time-dependent dipole–dipole interaction term is obtained from MD simulation.

We use two different inner BCs at the contact distance, σ , to solve for the coupled sets of equations. Namely, we use reflecting BC at $r = \sigma$, that takes into account the energy transfer effects and also the possibility that the transfer is not enhanced during an encounter, i.e.,

$$\left. \frac{\partial}{\partial r} \rho_{D^*A}(r, t) \right|_{r=\sigma} = 0 \quad \text{and} \quad \left. \frac{\partial}{\partial r} \rho_{A^*D}(r, t) \right|_{r=\sigma} = 0 \quad (22)$$

and the other inner BC used is the Smoluchowski absorbing BC,

$$\rho_{D^*A}(r, t)|_{r=\sigma} = 0 \quad \text{and similarly} \quad \rho_{A^*D}(r, t)|_{r=\sigma} = 0. \quad (23)$$

The outer BC at $r = \infty$ is given by

$$\lim_{r \rightarrow \infty} \rho_{D^*A}(r, t) = 1. \quad (24)$$

The BC at $r = \infty$ for ρ_{A^*D} distribution function is obtained after some simple manipulation⁷ and is given by [assuming that $g(r) = 1$]

$$\rho_{A^*D}(\infty, t) = 1. \quad (25)$$

The initial condition for $\rho_{D^*A}(r, t)$ is

$$\rho_{D^*A}(r, t=0) = \exp[-U_{D^*A}(r)/k_B T] = g(r). \quad (26)$$

In the absence of the solvent influence on the potential of mean force acting between the molecules, as we assume in this work (see below), the right-hand side of Eq. (26) is equal to 1. It is to be noted that separate temporal evolution of A^* and D starts only after the first forward transfer step from D^* to A such that some amount of A^* is formed. If we assume that first forward transfer step is δt then reverse transfer time scale is shifted δt time apart from the forward transfer time scale. In view of this fact the initial condition for ρ_{A^*D} is given by

$$\rho_{A^*D}(r, t=0 + \delta t) = 1. \quad (27)$$

This result is obtained after a similar manipulation that leads to Eq. (25).

Equations (8) and (9) with the above BCs can only be solved numerically. We employ the Crank–Nicolson finite difference scheme¹⁹ for this purpose. However, Eqs. (2), (8) and (3), (9) together with Eqs. (4) and (5) are a coupled set of equations and are solved by using the iterative method.^{7,20} The zeroth order initial ($t=0$) value of the rate constants were obtained from

$$k_Q^f(t) = \int_{\sigma}^{\infty} dr 4\pi r^2 S_{DA}(r) \rho_{D^*A}(r, t=0) = \frac{4\pi K_S^D R_{0f}^6}{3\sigma^3}$$

and

$$k_Q^r(t=0) = 0.$$

Extreme care was taken to make sure that the results were stable, accurate, and converged. Finally, the value of D^* number density thus obtained is normalized with respect to D^* number density at $t=0$. The normalized time-dependent number density of the D^* molecule represents its survival probability, $\eta_{D^*}(t)$ that can be compared with the ensemble averaged simulated survival probabilities [utilizing Eqs. (20) and (21)].

B. Molecular dynamics simulation

The algorithm to solve the Liouville formalism based Eq. (20) and the Eq. (21) obtained from first principle requires the fluctuating part of the equation in the form of trajectories of a fluid system containing a pair of pairwise interacting chromophores. This is basically a stochastic problem where one is interested in the configurational part of the problem in the phase space. Molecular dynamics simulation is on the other hand a deterministic method. The idea behind this methods is to use the intrinsic dynamics of the model to propagate the system. However, the scope of the stochastic methods is wide. Assuming that the present stochastic problem is a Markov process, we can equally well generate the trajectories of the molecules by molecular dynamics simulation techniques for the reason that the Markov process is the probabilistic analogue to the intrinsic dynamics. Therefore, in this work the trajectories were simulated by MD simulation technique²¹ of a Lennard-Jones fluid and could equally well be generated by Brownian dynamics simulation techniques.¹¹

TABLE I. Self-diffusion coefficients for a Lennard-Jones fluid in reduced units^a (with $\epsilon=m=\sigma=1$).

ρ^*	T^*	Self-diffusion coefficient
0.85	2.04	0.125
0.85	0.836	0.0393

^aReference 22.

The simulations of trajectories were carried out in a box, which contained 498 solvent molecules with one donor and one acceptor molecule embedded in it. The simulating system is characterized (in reduced units of Lennard-Jones parameters such that $\epsilon=m=\sigma=1$) by a density ρ^* and a temperatures T^* . The simulation step size in reduced units of time was taken be 0.001. Trajectories were generated at two different diffusing environments. The corresponding diffusion coefficients are given Table I. Solvent–solvent interaction was taken to be the same as solute–solvent interaction. Equation of motion for the particles were integrated using the velocity-Verlet algorithm. To mimic an infinite system which is relevant for comparisons with the many-body Smoluchowski equation, we use periodic BCs, i.e., the box is surrounded by replicas of itself. To find the interparticle distance, the minimum image convention is implemented in all the calculations. While calculating the transfer rates only reactants within a certain cutoff radius R_C (usually taken as half the box length), are considered. The medium outside the cutoff radius is included via a continuum approach.^{12,13} The transfer rates as given in Eqs. (6) and (7) which are same as those appeared in Eqs. (20) and (21) at a given instant of time, is given by

$$W_{\alpha}(r, t) = \begin{cases} \frac{1}{\tau_{0j}} \left[\frac{R_{0\alpha}}{r(t)} \right]^6 & \text{for } r < R_C \\ \frac{c}{\tau_{0j}} \left(\frac{R_{0\alpha}}{R_C} \right)^3 & \text{for } r > R_C \end{cases}, \quad (28)$$

where c is the reduced reactant concentration defined as

$$c = \frac{4\pi R_{0\alpha}^3}{3} \rho_j. \quad (29)$$

ρ_j is number density of the reactant j . For R_C =half the box length

$$W_{ga}(r, t) = \frac{0.523}{\tau_{0j}} \left(\frac{R_{0\alpha}}{R_C} \right)^6 \text{ for } r > R_C.$$

This spherical cutoff convention is valid only when

$$\frac{R_{0\alpha}}{R_C} < 1. \quad (30)$$

With these definitions in mind we now turn to the computation of our model in the weak dipolar coupling regime.

At each MD step the snapshots of the particle positions can be thought of as if their translational movements are “frozen.” Therefore, at each simulation time step Eqs. (20) and (21) for the Förster master rate of energy transfer can be solved following a finite difference technique. Conceptually

the calculation of the survival probability of the donor involves three consecutive steps. These are (i) trajectory generation for one donor and one acceptor by MD simulation, (ii) solution of Eqs. (20) and (21) at each MD step, and (iii) repetitions of steps (i) and (ii) for several other choices of donor and acceptor to obtain a well-averaged property. However, these sequential runs are only prohibitively large time consuming. Instead, aided by the prescription that all particles in the simulating system are equivalent and that counting of distance between a given pair of particles is independent of others, we have taken $>10^5$ pairs of the donor and the acceptor for a 500 particle simulating system and for a given pair the other particles are treated as solvent molecules. With this prescription the computer program was written and finally an average of the physically most interesting element, χ_1 and N_{D*} and over all the pairs at each time steps were made. The ensemble averaged χ_1 represents the survival probability of the donor, $\eta_{D*}(t)$ for a donor-donor situation. Similarly the normalized and ensemble averaged $N_{D*}(t)$ also represent $\eta_{D*}(t)$ for energy transfer between dissimilar partners.

It is important to note that apparently $[D^*]$ and $[A^*]$ that appear in Eqs. (2) and (3) are space independent whereas χ_1 and χ_2 in Eq. (20) and similarly N_{D*} and N_{A*} in Eq. (21) are dependent on the interparticle separation. However, a closer look into these equations [Eqs. (2) and (3)] reveal that they are dependent on $k_Q^f(t)$ and $k_Q^r(t)$ which in turn depends explicitly on the space dependent nonequilibrium pair distribution functions $\rho_{D^*A}(r,t)$ and $\rho_{A^*D}(r,t)$, respectively. Therefore, the dependence of $[D^*]$ and $[A^*]$ on the particle separation r is implicit in this theory. Moreover we do not directly identify $[D^*]$ and $[A^*]$ with χ_1 and χ_2 , rather as mentioned above an ensemble averaged χ_1 is compared with $[D^*]$. It is in this sense that the reaction-diffusion analog of Eqs. (20) and (21) are Eqs. (2) and (3).

In the strong dipolar regime (where the Förster transfer rate is not valid) for the donor-donor case, we make use of the Liouville result i.e., Eq. (18) and follow the same steps as stated in Sec. II and finally the correlation function, $\langle \chi_1(t) | \chi_1(t_0) \rangle$ was obtained in a single sweep. This correlation function bears the same meaning of the ensemble averaged survival probability as χ_1 , only here it is averaged in a different fashion. Several standard subroutines were obtained from Ref. 20. In all our subsequent results and discussion we use the reduced form of time in the units of $(m\sigma^2/\epsilon)^{1/2}$ such that $\epsilon=m=\sigma=1$ and the molecular diameter is taken to be the same as the Lennard-Jones parameter, σ .

IV. RESULTS AND DISCUSSION

After we obtain the time-dependent random donor-acceptor distance by molecular dynamics, we solve the Förster master rate Eqs. (20) and (21). Equation (21) can be used both for the irreversible ($W_r=0$) and the reversible processes. Finally an averaged survival probability of the donor is obtained. Equation (20) is rederived from the Liouville formalism in the weak dipolar interaction limit. Therefore, the survival probabilities that are obtained from Eq. (20)

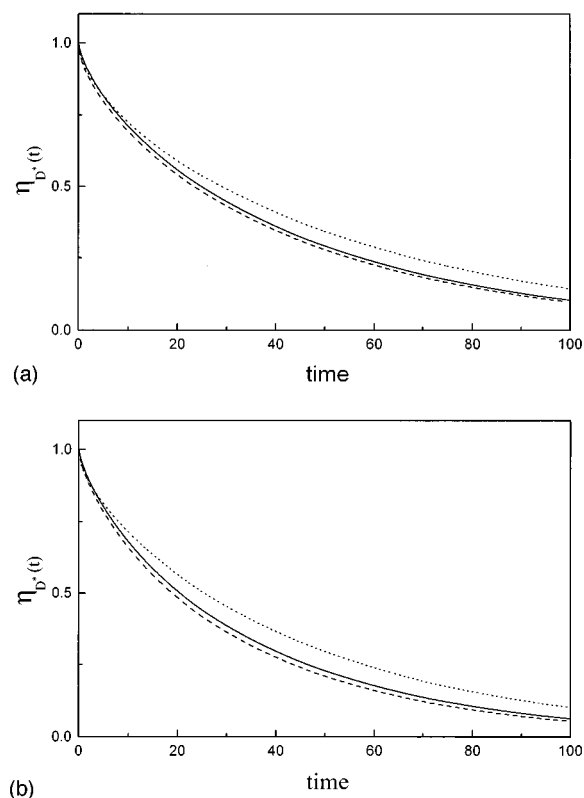


FIG. 1. (a) Survival probability of the donor obtained from Eq. (21) combined with MD simulations (\cdots), the reaction-diffusion formalism solved for reflecting boundary condition ($---$), and for the absorbing boundary condition ($—$) at contact at $D=2\times 0.0393$, $R_{0f}=3\sigma$, $R_{0r}=0$, $\tau_{0D}=\tau_{0A}=100$. (b) Same as (a) with $D=2\times 0.125$.

aided with the MD simulation are in fact Liouville formalism based results. On the other hand, although Eq. (21) is similar in structure as to Eq. (20) but the former was not obtained as such from the SLE formalism. However, the MD approach [that has been utilized in solving Eq. (21)] is like a very detailed mechanical description that the very complexity of such a process make it necessary to model the role of solvent through a friction like term in the Langevin equation to characterize the motion. That is the results obtained from Eq. (21) combined with MD simulations are in fact based on Fokker-Planck equation (corresponding to Langevin dynamics). Using the coupled set of dynamic equations [namely, Eqs. (2) and (8) coupled with Eqs. (3) and (9), Eqs. (4) and (5) being common to them] for the reaction-diffusion formalism we also solve for the normalized number density of the excited donor molecules. This latter result that also stands for the survival probability is then compared with the results obtained from Eqs. (20) and (21) combined with MD simulation techniques. In all the calculations we assume that at zero time only one excited donor and one ground state acceptor molecule is dissolved in a 500 particle system. Let us first consider the irreversible transfer process i.e., when the reverse transfer rate is set equal to zero.

Figure 1(a) shows the survival probability of the donor in an irreversible transfer process, obtained from solving Eq. (21) and from the reaction-diffusion formalism solved for

absorbing boundary [cf. Eq. (23)] as well as for the reflecting boundary [cf. Eq. (22)] condition in a diffusing medium that corresponds to a self-diffusion coefficient of the individual chromophore equated to 0.0393. Figure 1(b) represents the same irreversible transfer at a less viscous medium with self-diffusion coefficient of the chromophores equal to 0.125.

From Figs. 1(a) and 1(b) it can be seen that the rate of long-range energy transfer obtained from reaction-diffusion formalism is substantially higher than that obtained from the simulated results. This result is in accord with the earlier results^{23–25} on the solution of the Fokker–Planck equation for absorbing BC and the rate coefficient thus obtained can be substantially smaller than that of the diffusion equation. However, the latter results^{23–25} were all obtained for collisional transfer in contrast to the present long-range interaction.

The basic model underlying the solutions of Eqs. (20) and (21) with the particle trajectories obtained from MD simulation is somewhat similar to the simplest position dependent rate of Szabo.²⁶ Szabo has considered a simple quenching model where the sink function is assumed to be inverse of a constant and finite nonradiative lifetime value within a range from contact distance to a certain cutoff radius, and is zero (lifetime is infinite) outside the cutoff radius. The resulting reaction-diffusion equation was solved analytically²⁶ assuming a reflecting boundary at contact. Similar to this, in our model simulation at the Lennard-Jones parameter, σ (which has also taken to be equal to molecular diameter) the particles face a steep repulsive potential i.e., the model assumes a reflecting wall at σ . To complete the correspondence to the Szabo's model, the present model also imposes a position dependent rate within a distance from σ to R_c but unlike the Szabo's model the sink function is finite outside the cutoff radius but is negligible since $R_0/R_c < 1$. The analytical solution of Szabo's model²⁶ clearly shows that the time-dependent rate coefficient comprises of a "static quenching" part between σ and R_c and a diffusion dependent dynamic quenching part. Szabo has also shown that the steady state fluorescence intensity ratio in the presence and absence of quencher, consists of a static quenching and a diffusion dependent term. The latter term has been found to be identical to that obtained from solving the diffusion equation for Collins–Kimball (CK) or radiative BC (Ref. 27) at R_c . Szabo's treatment also gives²⁶ a physical interpretation of the intrinsic rate constant that is used in CK BC and shows that this rate constant can be a function of diffusion coefficient and the sink function parameters.

The energy transfer sink function is certainly more complicated than that of Szabo's consideration.²⁶ And no analytical solution for such a reaction-diffusion equation is as yet known valid for all time and all diffusing environment. Sipp and Voltz (SV) (Ref. 28) has considered this problem but to make the mathematical treatment simpler they have assumed a slow and a fast diffusion time scale relative to the transfer rate characterized by a parameter X_0 ,

$$X_0 = \frac{1}{2} \left[\frac{R_0}{(D\tau_0)^{1/2}} \right] \left(\frac{R_0}{\sigma} \right)^2. \quad (31)$$

In both the diffusion limit ($X_0 \ll 1$, fast diffusion; $X_0 \gg 1$, slow diffusion) SV has obtained the expression for the time-dependent rate coefficient and have identified a reaction length within which the static quenching takes place and beyond which a standard diffusion model applies. The reaction length has also been found to be a function of energy transfer parameters and diffusion coefficient of the medium. In view of this and the discussion in the preceding paragraph one can argue that in the present simulation model we are solving the Förster master rate equation such that static reaction predominates below a certain characteristic cutoff distance (cf. reaction length) beyond which a diffusion formalism applies with a radiative BC at the cutoff radius. And all these events are taking place in phase space. It is to be mentioned that since the concentration of the quencher species [$\rho_A^* = \rho^*(N_A/N) = 0.0017$] is low, the effects of static quenching will only be negligibly small.

As stated earlier the results obtained from Eq. (21) combined with MD techniques are essentially Fokker–Planck equation^{29,30} based results. In the time scale which is long compared to the "velocity relaxation" time of the particles the Fokker–Planck equation reduces to the Smoluchowski diffusion equation.^{23–25,29} In a medium with higher viscosity and therefore with smaller velocity relaxation time these two equations will correspond closely to each other even at an earlier time. In presence of a reaction, in a medium with higher viscosity (i.e., high friction limit) the CK BC reduces to Smoluchowski absorbing BC. In other words for the CK BC to apply, the reaction has to be slow as compared to diffusion. Based on this we expect that the simulated survival probabilities will behave closely to those obtained by solving the reaction-diffusion equation with an absorbing BC at a higher viscous medium. In a medium with higher diffusion coefficient the comparison will certainly be poor.

For the model parameters values in Figs. 1(a) and 1(b) X_0 values are 4.8 and 2.7, respectively. That is, the situation in Fig. 1(a) is more towards the slow diffusion (higher friction) and fast reaction limit than that in Fig. 1(b). Therefore, the simulated results compares relatively better with the reaction-diffusion result in Fig. 1(a) than in Fig. 1(b). The poor performance of the reflecting BC results is quite obvious from the long-range transfer rate coefficient as appeared in Eq. (4). An improvement over the present version of the reaction-diffusion equation would have been to incorporate the solvent influence on the potential of mean force [$U(r)$] between the two molecules. However, since the reaction is long-range, the influence of the inclusion of relatively short-range $U(r)$ on the rate of transfer is small²⁸ specially in the slow diffusion (fast reaction with larger R_0) regime. It is important to note that the Crank–Nicolson method of solving the coupled set of reaction-diffusion equation is very sensitive towards the temporal and spatial step size, and the necessary condition for convergence of calculation depends much on the excitation transfer parameters and on the initial number densities of the reactants. To attain the convergence of the results we have reduced the temporal and spatial step size significantly. For a given converged result we have checked its accuracy by repeating the calculation after halv-

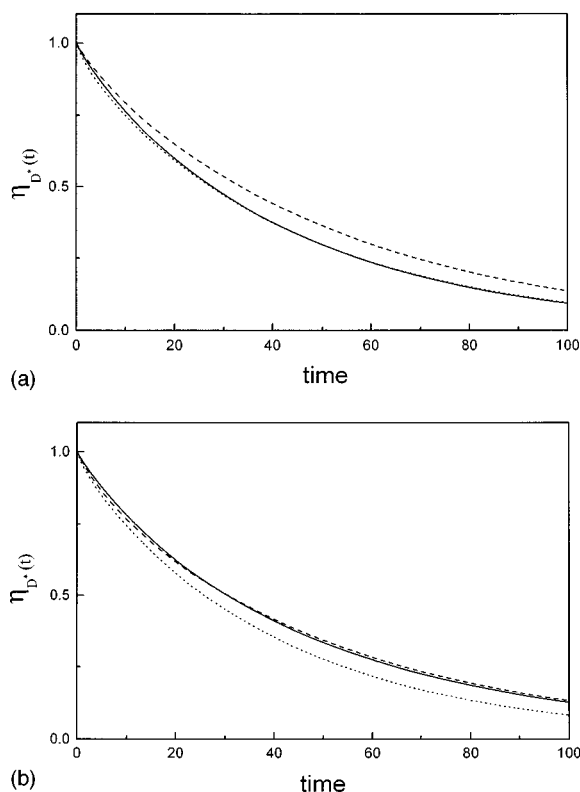


FIG. 2. (a) Survival probability of the donor for the reversible reaction obtained from Eq. (21) combined with MD simulations (\cdots), the reaction-diffusion formalism solved for reflecting boundary condition ($-\cdot-$), and for absorbing boundary condition ($—$) at $D=2 \times 0.0393$, $R_{0f}=2\sigma$, $R_{0r}=1.5\sigma$, $\tau_{0D}=50$, $\tau_{0A}=100$. (b) Same as (a) for $D=2 \times 0.125$.

ing the temporal and spatial step size. Therefore, the theoretical results in above for the irreversible reactions and in what follows for the reversible reactions can be treated as exact results.

For reversible reactions the situation is evidently more complex. This is because the transient effects induced by the diffusion of the medium are occurring repeatedly in both directions of energy flow.⁷ The parameter X_0 [cf. Eq. (31)] that differentiates between the slow and the fast diffusion relative to the reaction rate will obviously have a different functional form including the forward and the reverse transfer parameters and diffusion coefficient of the medium. However, the basic idea behind the slow and the fast diffusion conditions at each direction of the energy flow will still hold. Bearing this in mind we have calculated the survival probability of the donor when $R_{0f}=2\sigma$, $R_{0r}=1.5\sigma$, $\tau_{0D}=50$, $\tau_{0A}=100$. The results are plotted in Fig. 2 for (a) $D=2 \times 0.0393$ and (b) $D=2 \times 0.125$. These parameter values corresponds to $X_0=2.02$ (forward transfer) and 0.602 (reverse transfer) when $D=2 \times 0.0393$. For $D=2 \times 0.125$ the X_0 values are 1.13 (forward transfer) and 0.337 (reverse transfer). That is both in Figs. 2(a) and 2(b) the situation represents a slow diffusion relative to the forward transfer rate and a fast diffusion relative to the reverse transfer rate. Northrup and Hynes²⁵ has considered reversible reaction in a space where the inner and outer regions are separated by a

boundary layer. They have shown for such situation the probability distribution function of the reactants will follow a radiative BC. In the light of this and in view of the foregoing analysis on an irreversible reaction we can say that the simulated survival probabilities in Figs. 2(a) and 2(b) represent a solution of the Förster master rate Eq. (21) of reversible reaction with radiative (CK) BC modulated by the diffusion and fluctuation in the phase space.

In Fig. 2(a) the reverse process is in the fast diffusion (slow reaction) limit. As stated above for such conditions the reaction-diffusion equation solved for absorbing/reflecting BC will give rise to a higher rate of transfer as compared to that in CK BC. This leads to a higher rate of back transfer and thus the survival probability of the donor in a reversible reaction will be higher than the simulated results when plotted with respect to time. Once again the absorbing BC results as compared to the reflecting BC will be closer to the simulated values. This is exactly observed in Figs. 2(a) and 2(b). In Fig. 2(a) the absorbing BC result overlaps with the simulation result. But this agreement is only fortuitous, no special physical reason should be attached to it. In Fig. 2(b) the comparison is poor because of the fact that the results are obtained in a medium with a lower friction coefficient.

To study the other possibility of coupling of transfer and diffusion in reversible reaction we have interchanged the transfer rate parameters of Fig. 2, between the donor and the acceptor. The results are plotted in Fig. 3 for (a) $D=2 \times 0.0393$ and (b) $D=2 \times 0.125$. The situation depicts that the forward transfer rate is slower than the diffusion rate and vice versa for the reverse step. The results in these figures show that the absorbing BC results overlap with the reflecting BC results. The reason is that the forward transfer parameter ($R_{0f}=1.5\sigma$) is low and the acceptor lifetime is half of the donor lifetime. The result is that the quantum of energy transferred from the donor to the acceptor is low and the acceptor decays to the ground state before it gets a chance to reverse transfer. The overall impact on the survival probability is that the donor decays following almost its natural decay with a lifetime equal to 100. In such situations, as one would expect that the simulation results and the reaction-diffusion results will agree well at all times. It is important to note that for such fast-slow diffusion combination of forward-reverse transfer, by reducing the diffusion coefficient of the medium by a factor of 10^2 , one arrives at a slow-slow diffusion combination. And the donor is found to decay differently from its natural decay.⁷ However, in the present work we are restricted to a lowest self-diffusion of 0.0393 reported in Ref. 22 for which Fig. 3(a) is plotted.

We now turn our discussion to the donor-donor case of reversible energy transfer. That is we use Eq. (20) (SLE formalism based result) combined with MD techniques. The Liouville equation combined with MD techniques is again a very complicated description of the motion of individual reactants. This necessitates to model the role of solvent molecule through a stochastic description in terms of the probability distribution of position and velocity. And such a complicated system can be well described by the Fokker-Planck equation.^{29,30} In Fig. 4 we display the results for

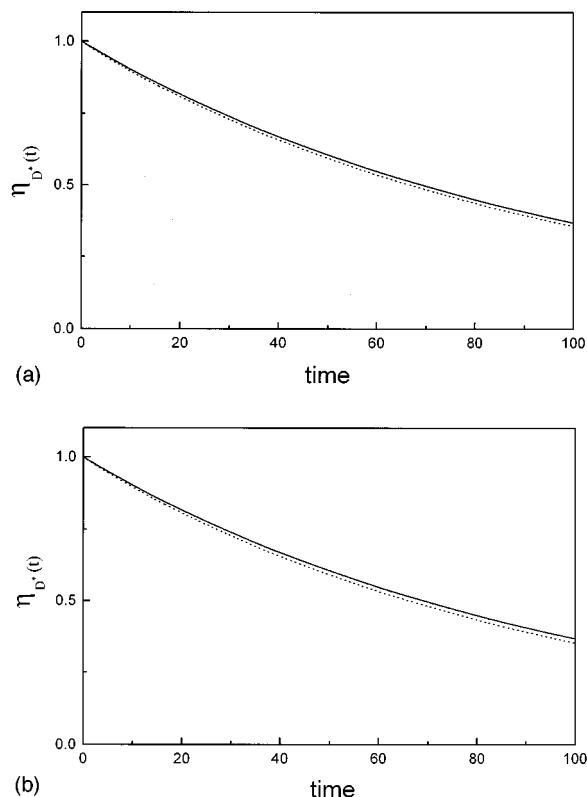


FIG. 3. (a) Survival probability of the donor for the reversible reaction obtained from Eq. (21) combined with MD simulations (\cdots), the reaction-diffusion formalism solved for the reflecting boundary condition ($-\cdot-$), and for the absorbing boundary condition ($—$) at $D=2\times 0.0393$, $R_{0f}=1.5\sigma$, $R_{0r}=2.0\sigma$, $\tau_{0D}=100$, $\tau_{0A}=50$. (b) Same as (a) with $D=2\times 0.125$.

$R_{0f}=R_{0r}=2.0\sigma$ and $\tau_{0D}=\tau_{0A}=100$ at (a) $D=2\times 0.0393$ and (b) $D=2\times 0.125$. Based on the arguments presented above in connection with the irreversible/reversible energy transfer between dissimilar reactant partners we can calculate the X_0 values for such a pair and compare the theoretical results with the simulated results. These parameters give rise to X_0 values equal to (a) 1.42 and (b) 0.8. That is, in case (a) the forward–reverse processes are relatively in the slow diffusion (fast reaction) regime than in case (b). This view supports the fact that the discrepancy between the simulated results and the reaction-diffusion result is relatively smaller in the case of Fig. 4(a) (higher friction) than in the case of Fig. 4(b), where the diffusing medium offers a lower friction.

Let us now consider the energy transfer in a strong dipolar interaction limit. As we have already mentioned, the Förster rate equation approach that we have considered so far in this section, will not apply in this limit. The SLE approach as given by Eq. (18), on the other hand, is a powerful alternative in this interaction limit.¹¹ For this we solve Eq. (18) with the stochastic fluctuating part (in the expression for dipole–dipole interaction Hamiltonian) are obtained as earlier from the MD simulation. The algorithm¹¹ to solve the SLE equation is discussed in Sec. II for the donor–donor case of reversible transfer. The parameters that enter into the full form of the Liouville formalism are taken to be $\tau_{0D}=40$, $T_{2,D}=0.1$. The calculated time correlation functions

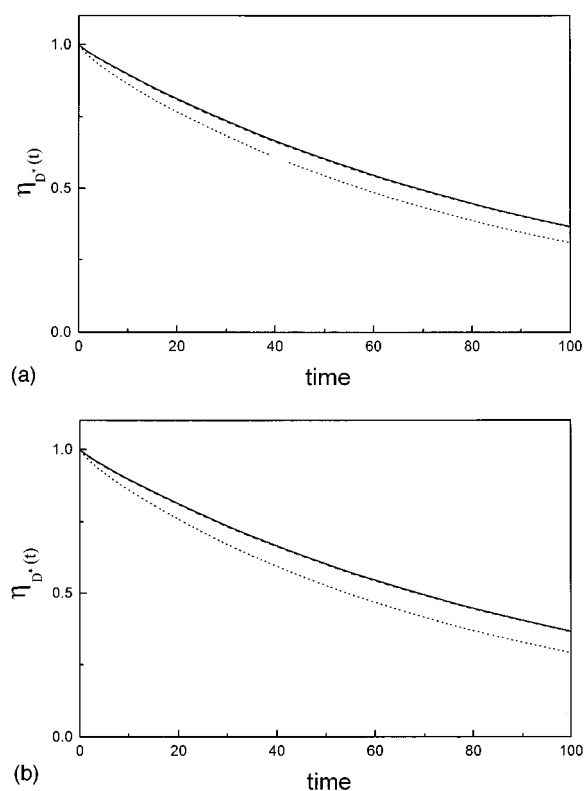


FIG. 4. (a) Survival probability of the donor for the reversible reaction obtained from Eq. (20) combined with MD simulations (\cdots), the reaction-diffusion formalism solved for the reflecting boundary condition ($-\cdot-$), and for the absorbing boundary condition ($—$) at $D=2\times 0.0393$, $R_{0f}=R_{0r}=2.0\sigma$, $\tau_{0D}=\tau_{0A}=100$. (b) Same as (a) with $D=2\times 0.125$.

representing the survival probabilities of the donor for three different values of the time invariant part of the dipole–dipole interaction Hamiltonian are plotted in Fig. 5. It is to be mentioned that all these parameter values are in the reduced unit of frequency such that $\epsilon=m=\sigma=1$. The results in this figure are for $D=2\times 0.125$. However, in this strong interaction limit the survival probabilities are found to be almost invariant with respect to viscosity of the medium similar to the result obtained in Ref. 11. As can be seen from the figure that with the increase in dipolar interaction

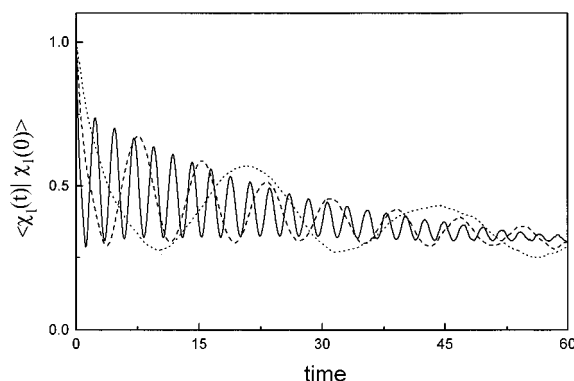


FIG. 5. Donor–donor reversible energy transfer in the strong dipolar coupling regime for $(\mu_A\mu_D/4\pi\epsilon_0\sigma^3)=10(\cdots)$; $30(-\cdot-)$; $100(—)$.

strength the oscillation in the correlation function increases, but at long time the oscillations dampens out such that the donor with different interaction strengths decays in a similar fashion. The oscillatory behavior suggests the rapidity of the quanta of energy flow between the donor–donor pair; higher the interaction strength more rapid is the bidirectional flow of quantum of energy.

V. CONCLUSIONS

In this work, the algorithm that has been developed previously by Fedchenia and Westlund¹¹ to solve the SLE for the electronic excitation transfer between a donor–donor pair has been utilized to study the effects due to translational diffusion in Lennard-Jones fluid. However, for the obvious difficulty in connecting the eigenvalues of the matrix elements of the density matrices of the individual chromophores and the dipolar interaction strength with the Förster radius, the algorithm cannot be used as such for the comparison sake with the theoretical predictions. This is more so for the reason that the SLE formalism involves mixed coupled states of the density matrix elements (χ_3 and χ_4) of the individual chromophores in contrast to the Förster mechanism. Fortunately, the Förster master rate equation of excitation population can be rederived from the Liouville formalism in the weak perturbation (dipolar interaction) limit.¹⁰ Using this argument and the fact that at each MD snapshot, the distance between a donor–acceptor pair, as if their translational motions are frozen, the fluctuating Förster rate is obtained at each MD step.

The Förster master rate Eq. (21) for irreversible/reversible transfer of energy between dissimilar chromophore partner is similar in structure with that in Eq. (20). Solution of Eqs. (20) and (21) combined with MD simulation techniques can be viewed as the solution of the Fokker–Planck equation. Comparison of the results obtained from this formalism with those obtained from the reaction-diffusion formalism solved for the absorbing BC clearly shows the effects due to variation of the medium friction coefficient both in the irreversible and in the reversible case of excitation transfer. The similarity of results obtained by two different techniques is a manifestation of the unified nature of derivation of the generalized Brownian motion theory.¹⁷ The Liouville equation is the starting point. From this the stochastic theory used by Langevin to treat the Brownian motion can be obtained. This latter theory is phenomenological in nature and can well describe the transport processes in fluids. The nature of MD approach necessitates to model the role of solvent molecules through a frictionlike term in the Langevin equation. It is well known that the Langevin dynamics reduces to solving the diffusion equation in the high friction limit.^{23–25,29} However, in contrast to the collisional reaction model,^{15,16,23–25} where much of the molecular nature of the reacting system is over looked, the present model with a sink function approach is more physical

in the sense that this model gives rise to a well defined reaction length²⁸ distinctly different from the collisional radius. The important aspect to note is that, even in such situation the Liouville based results reduces to diffusion formalism at high friction limit.

In view of the earlier result on hard-sphere liquid on collision reaction,^{15,16} a modest goal of the present reaction-diffusion formalism will be the use of a more realistic CK BC after the incorporation of solvent influence on the potential of mean force into the formalism. This can only be achieved once the nature of the intrinsic rate coefficient and the potential of mean force, are sufficiently known.

ACKNOWLEDGMENTS

It is a pleasure to thank Dr. J. P. Mittal, Dr. C. Gopinathan, and Dr. T. Mukherjee for their constant encouragement during the entire course of this work. The author is also indebted to J. P. Mittal and H. Pal for many stimulating discussions.

- ¹Th. Förster, *Ann. Phys.* **2**, 55 (1948).
- ²D. L. Dexter, *J. Chem. Phys.* **21**, 836 (1953).
- ³S. A. Rice, *Comprehensive Chemical Kinetics* (Elsevier, New York, 1985), Vol. 25.
- ⁴N. N. Lukzen, A. B. Doktorov, and A. I. Burshtein, *Chem. Phys.* **102**, 289 (1986).
- ⁵A. I. Burshtein and N. N. Lukzen, *J. Chem. Phys.* **103**, 9631 (1995).
- ⁶K. Sienicki and W. L. Mattice, *J. Chem. Phys.* **90**, 6187 (1989).
- ⁷T. Bandyopadhyay, *J. Chem. Phys.* **106**, 5049 (1997).
- ⁸S. Lee and M. Karplus, *J. Chem. Phys.* **86**, 1883 (1987).
- ⁹A. Szabo, *J. Chem. Phys.* **95**, 2481 (1991).
- ¹⁰Per-Olof Westlund and H. Wennerström, *J. Chem. Phys.* **99**, 6583 (1993).
- ¹¹I. Fedchenia and Per-Olof Westlund, *Phys. Rev. E* **50**, 555 (1994).
- ¹²S. Engström, M. Lindberg, and L. B. A. Johansson, *J. Chem. Phys.* **89**, 204 (1988).
- ¹³S. Engström, M. Lindberg, and L. B. A. Johansson, *J. Chem. Phys.* **96**, 7528 (1992).
- ¹⁴W. Dong, F. Baros, and J. C. Andre, *J. Chem. Phys.* **91**, 4643 (1989).
- ¹⁵H. X. Zhou and A. Szabo *J. Chem. Phys.* **95**, 5948 (1991).
- ¹⁶T. Bandyopadhyay, *J. Chem. Phys.* **102**, 9557 (1995).
- ¹⁷(a) S. Nordholm and R. Zwanzig, *J. Stat. Phys.* **13**, 347 (1975); (b) L. S. García-Colín and J. L. D. Rio, *ibid.* **16**, 235 (1977).
- ¹⁸(a) R. H. Pantell and H. E. Puthoff, *Fundamentals of Quantum Electronics* (Wiley, New York, 1969); (b) C. N. Banwell and H. Primas, *Mol. Phys.* **6**, 225 (1963).
- ¹⁹W. H. Press, B. P. Flannery, S. A. Teukolsky, and W. T. Vetterling, *Numerical Recipes* (Cambridge University Press, Cambridge, 1986).
- ²⁰M. Yang, S. Lee, K. J. Shin, K. Y. Choo, and D. Lee, *Bull. Korean Chem. Soc.* **13**, 325 (1992).
- ²¹M. P. Allen and D. J. Tildesley, *Computer Simulation of Liquids* (Oxford University Press, Oxford, 1987).
- ²²J. A. Leegwater, *J. Chem. Phys.* **94**, 7402 (1991).
- ²³(a) S. Haris, *J. Chem. Phys.* **78**, 4698 (1983); (b) **72**, 2659 (1980); (c) **75**, 3103 (1981).
- ²⁴J. T. Hynes, R. Kapral, and G. M. Torrie, *J. Chem. Phys.* **72**, 177 (1980).
- ²⁵S. H. Northrup and J. T. Hynes, *J. Chem. Phys.* **68**, 3203 (1978).
- ²⁶A. Szabo, *J. Phys. Chem.* **93**, 6929 (1989).
- ²⁷F. C. Collins and G. E. Kimball, *J. Colloid Sci.* **4**, 425 (1949).
- ²⁸(a) B. Sipp and R. Voltz, *J. Chem. Phys.* **79**, 434 (1983); (b) **83**, 157 (1985).
- ²⁹S. Chandrasekhar, *Rev. Mod. Phys.* **15**, 1 (1943).
- ³⁰H. Risken, *The Fokker–Planck Equation Methods of Solution and Applications* (Springer, Berlin, 1984).